Advanced Drug Delivery Reviews 64 (2012) 1639–1649

Contents lists available at SciVerse ScienceDirect

Advanced Drug Delivery Reviews

journal homepage: www.elsevier.com/locate/addr

Compact, power-efficient architectures using microvalves and microsensors, for intrathecal, insulin, and other drug delivery systems ☆

Tao Li [a,*], Allan T. Evans [a,1], Srinivas Chiravuri [b], Roma Y. Gianchandani [c], Yogesh B. Gianchandani [a]

[a] Department of Electrical Engineering and Computer Science, University of Michigan, 1301 Beal Ave., Ann Arbor, MI, 48109-2122, USA
[b] Department of Anesthesiology, University of Michigan, 1500 East Medical Center Drive, Ann Arbor, MI, 48109-5048, USA
[c] Department of Internal Medicine, University of Michigan, Domino's Farms, 24 Frank Lloyd Wright Drive, Room G1625, Ann Arbor, MI, 48109, USA

ARTICLE INFO

Article history:
Received 28 September 2011
Accepted 3 May 2012
Available online 8 May 2012

Keywords:
Multidrug delivery
Microvalve manifold
Liquid flow control
MEMS
Implantable drug pump
Wearable drug pump
Power transfer
Piezoelectric

ABSTRACT

This paper describes a valve-regulated architecture, for intrathecal, insulin and other drug delivery systems, that offers high performance and volume efficiency through the use of micromachined components. Multi-drug protocols can be accommodated by using a valve manifold to modulate and mix drug flows from individual reservoirs. A piezoelectrically-actuated silicon microvalve with embedded pressure sensors is used to regulate dosing by throttling flow from a mechanically-pressurized reservoir. A preliminary prototype system is demonstrated with two reservoirs, pressure sensors, and a control circuit board within a 130 cm^3 metal casing. Different control modes of the programmable system have been evaluated to mimic clinical applications. Bolus and continuous flow deliveries have been demonstrated. A wide range of delivery rates can be achieved by adjusting the parameters of the manifold valves or reservoir springs. The capability to compensate for changes in delivery pressure has been experimentally verified. The pressure profiles can also be used to detect catheter occlusions and disconnects. The benefits of this architecture compared with alternative options are reviewed.

Contents

☆ This review is part of the *Advanced Drug Delivery Reviews* theme issue on "Emerging Micro- and Nanotechnologies for the Development of Novel Drug Delivery Devices and Systems".

* Corresponding author at: 1301 Beal Avenue, Ann Arbor, MI, 48109-2122, USA. Tel.: +1 734 615 7983; fax: +1 734 763 9324.
E-mail addresses: litz@umich.edu (T. Li), evansall@umich.edu, allan.evans@pnl.gov (A.T. Evans), chiravun@umich.edu (S. Chiravuri), romag@umich.edu (R.Y. Gianchandani), yogesh@umich.edu (Y.B. Gianchandani).
[1] Present address: National Security Directorate, Pacific Northwest National Laboratory, 902 Battelle Blvd, PO Box 999 MSIN K5-17, Richland, WA 99352, USA.

0169-409X/$ – see front matter © 2012 Elsevier B.V. All rights reserved.
doi:10.1016/j.addr.2012.05.002

1. Disease incidence and the need for pumps

Drug delivery pumps have been commonly used in clinic treatment of a number of diseases and medical disorders. For example, intrathecal drug delivery is generally provided by pumps that are implanted; insulin delivery is often provided by pumps that are worn externally. Despite the differences in usage, both types of pumps have common features that can benefit from microsystems technology. Prior to addressing the system challenges, it is helpful to review the usage of these pumps and the currently available options.

1.1. Chronic pain and intrathecal drug delivery

Over 100 million people in the United States are afflicted by chronic pain with annual treatment costs exceeding $100 billion [1,2]. Defined by the International Association for Study of Pain (IASP) as symptoms lasting 6 months or more, chronic pain commonly manifests in the form of back pain, headache, arthritis, cancer pain, neuropathic pain resulting from nerve injuries (complex regional pain syndrome), and others like failed back surgery syndrome [3]. Both pharmacological and non-pharmacological treatment methods have been used for chronic pain management [4,5]. The use of various drugs (non-steroidal anti-inflammatory drugs, muscle relaxants, opioids), physical therapy, and psychological counseling are among the conservative non-invasive options. These measures are not effective for all patients; side effects sometimes develop as well. More advanced treatment options, such as nerve blocks, steroid injections, neurolysis, neurostimulation and intrathecal drug delivery devices (IDDD) [6–11], are considered in these situations.

Intrathecal drug delivery is used for treating pain and spastic symptoms. It decreases the need for oral analgesics and the associated side effects [12,13]. The benefits of IDDDs include potent analgesic response with stable therapeutic drug levels, decreased latency, increased duration of action, and decreased pharmacological complications like sedation, constipation, nausea and vomiting. The effectiveness of the implanted drug delivery pumps is derived from direct access into the cerebrospinal fluid (CSF) in the intrathecal space: about 1/300th of the amount of medication used in oral delivery provides the same level of analgesia [14,15]. The central action on opioid receptors allows intrathecal opioids to significantly affect pain anywhere inferior to the cranial nerves. These medications have a low coefficient of distribution in lipids and do not cross the blood–brain barrier, resulting in prolonged action. This is a major advantage for patients who require higher order mental faculties and control [14].

Intrathecal opioid administration has been utilized for chronic pain control for over 20 years [16,17]. Demand for multi-drug capabilities in IDDDs continues to arise as pain-relieving drugs evolve. The efficacy of polyanalgesia for acute pain management is well established in literature [18,19]. Although based upon limited trials with a small sample size, consensus opinion is that for chronic pain poly-drug approaches offer significant benefits [20,21]. In particular, intrathecal polyanalgesia employing opioids combined with non-opioid analgesics can have a higher degree of efficacy in patients with complex chronic pain of spinal origin, reducing major drug-related complications [4,22]. For instance, the addition of clonidine intrathecally to a low dose of opioid was effective in treating neuropathic pain which was refractory to opioid alone [23]. In another example, intrathecal morphine, when combined with stable doses of intrathecal Ziconatide, which is an intrathecal analgesic, reduces pain in patients with previously suboptimal pain relief on Ziconatide monotherapy [24,25]. The combination of opioid agonist/antagonist may prove beneficial in the reduction of opioid induced hyperalgesia from high dose intrathecal morphine [26–28]. All these call for a multi-chamber IDDD to maximize opportunities to combine currently used analgesics in a manner that is not possible with single-drug devices.

1.2. Diabetes and insulin delivery

Diabetes mellitus is one of the leading causes of death and disability in the world; it affects at least 285 million people [29,30]. In 2050 its prevalence in the United States is expected to increase from the current level of 1 in 10 adults to between 1 in 5 and 1 in 3 adults [31]. Additionally the incidence of diabetes is increasing for those below the age of 20 years [31]. Diabetes mellitus is a metabolic disorder that results from either the absolute deficiency of insulin (Type 1 diabetes mellitus) or resistance to the action of insulin (Type 2 diabetes mellitus). The diagnosis of diabetes mellitus is indicated by two confirmed levels of fasting blood glucose concentrations higher than 126 mg/dL (6.9 mmol/L) [32,33], or hemoglobin A1c of $\geq$6.5% or two-hour postprandial glucose of 200 mg/dL with symptoms. Complications of diabetes affect the macrovascular system, i.e. the heart and large blood vessels, and the microvascular system, causing kidney failure, nerve damage, or blindness.

Diabetic complications, particularly the microvascular complications, can be greatly reduced by stringent glycemic control [34,35]. The drugs used to treat diabetes are insulin and oral hypoglycemic agents (OHA). For patients with Type 1 diabetes, insulin is the mainstay of therapy. In Type 2 diabetes, the initial years after diagnosis may be managed by OHAs, but patients may eventually require insulin. Hence, all Type 1 diabetes patients and a significant group of Type 2 patients eventually use multiple daily injections of insulin: one or two injections of basal or long-acting insulin and several injections of bolus or short-acting insulin with each meal, for a total of 4–5 injections per day. The advent of insulin pen devices and ultrafine needle technology has improved the quality of life for the insulin-requiring population, but it still remains a complicated therapy and compliance with several shots a day is a significant patient burden. An effective option currently for the Type 1 population and in the future for Type 2 patients, could be the insulin pump technology for subcutaneous continuous insulin infusion. A simple and inexpensive pump could make a considerable difference in glucose and complications control, patient compliance and quality of life.

The capability of multi-hormone delivery in diabetes therapy has recently been investigated and confirmed as a desirable form of treatment. For example, glucagon, known as anti-insulin, has been investigated in combination with insulin in patients with Type 1 diabetes. Glucagon is normally produced by islet cells, and is present in Type 2 patients but not in Type 1 patients. Together, insulin and glucagon provide a closed-loop control mechanism for blood glucose levels. Delivery of both hormones as dictated by a glucose monitoring device can thus minimize insulin overdose and hypoglycemia [36]. It is also known that diabetes patients who require insulin are deficient in amylin. This is another pancreatic hormone which enhances insulin function, controls the rate of postprandial glucose and satiety. Insulin and amylin are co-secreted by the pancreatic beta cells; the ratio of these hormones is 20:1 in the peripheral circulation [37]. The two hormones together help stabilize blood glucose levels; amylin enhances functions of insulin by controlling postprandial glucagon spikes after meals, and reduces body weight. A device capable of multi-hormone delivery which could potentially mimic the natural physiology of the pancreas and additionally simplify dosing of insulin could change the diabetes treatment paradigm.

2. Current technology

2.1. Intrathecal drug delivery systems

With advances in technology, sophisticated intrathecal drug delivery systems have been developed to administer drugs into the CSF on a continuous basis [4,16,17,22,26–28,38–43]. Many of these systems are designed for implantation. These pumps are generally disk-shaped, range from 100 to 180 cm^3, and include a single drug reservoir. The

pumps are implanted underneath the skin of the abdomen between the skin and muscle tissue, and may be sutured to the fascia above the abdominal muscles. A catheter is inserted into the intrathecal space under fluoroscopy and secured to the thoracolumbar fascia. The other end is tunneled underneath the skin to the abdomen where it is connected to the implanted pump.

There are two categories of intrathecal drug pumps: active systems which are programmable, and passive systems with a constant preset flow rate. Several companies have developed intrathecal drug pumps in both categories (Table 1). Passive systems, such as IsoMed® from Medtronic and CODMAN® 3000 from Codman & Shurtleff, typically use a battery-free design, provide long implant life, and require no battery-replacement surgeries compared to active pumps [44,45]. However, the flow rate is restricted to one of a few preset delivery rates, and after implantation drug dosing can only be adjusted by varying the concentration of the medication. Active systems, such as SynchroMed® II and EL series from Medtronic [46,47], offer programmability. In these, a peristaltic pump is controlled by a microcontroller (μC) that can be programmed for different infusion modes (bolus, multi-step bolus, continuous, etc.) and delivery rates according to patient needs. The battery life depends on the infusion rate, and typically exceeds 5.5–7 years at a delivery rate of 0.9 mL/day.

All IDDDs include components other than the drug reservoir, reducing the fractional volume of the unit that may be occupied by the drug itself; this fractional volume is considered the volume efficiency ratio (VER). Passive systems traditionally have VERs ranging from 17 to 35% (Table 1) due to sophisticated pressurizing mechanisms that maintain a relatively constant reservoir pressure to generate a constant flow rate. Conventional active systems have VERs less than 26% (Table 1) because of the sizes of a peristaltic pump, a control circuit and a battery typically required for active control.

An alternative architecture that uses throttle valves to control flow from pressurized reservoirs allows a higher VER and overall compactness by obviating the pump, while still preserving the versatile delivery capabilities of an active system (Fig. 1) [48,49]. As discussed in more detail in Section 3, this architecture uses actively-controlled microvalves with embedded microsensors to precisely regulate drug dosage and delivery rate. This allows greater VER and customization of the delivery pattern. In addition, the use of servo-controlled flow rates helps reduce dosage errors and results in a safer implantation. The piezoelectric microvalves also promise a low-power operation. A preliminary implementation of this architecture has a 40 mL reservoir and a total size of 130 cm^3, resulting in a VER of 30.7% even at this early stage of development [48]. The embedded pressure sensors allow for dosing control and regulation with negligible impact to the system VER. The same sets of sensors may also be used for detection of catheter blockage or detachment, as well as residual volume in the reservoir.

This architecture is also appealing for multi-drug delivery systems. As discussed in Section 1.1, intrathecal delivery of multiple drugs is utilized in clinical practice when mono-drug therapy with opioids fails, either due to tolerance, opioid non-responsiveness (neuropathic pain) and/or hyperalgesia [38,39]. Typically a mix of an opioid, like morphine, and a local anesthetic is used for this. Currently these drugs are manually mixed and loaded in a single-reservoir IDDD for simultaneous delivery into the spinal fluid [4,40,41]. This imposes limitations on the type and concentration of drugs that can be administered. Long-term drug stability, interaction between mixed medications, and facility requirements all present challenges to the availability of compound mixtures [42]. Additionally, change in the delivery ratio of the mixed medications, which can happen more frequently during the early adjustment phase of an implant, requires the pump and the delivery catheter to be completely emptied and refilled with the new mixture. This can result in greater infection risks due to an increased frequency of needle punctures [50]. A system with multiple, independently-regulated, drug reservoirs can improve analgesic efficacy, reduce treatment cost, and ultimately improve patient satisfaction [42]. Compared with conventional active and passive IDDD architectures, the valve-regulated device architecture accommodates multi-drug delivery for combination therapy in a manner that will improve drug synergistic effects. For example, it allows the delivery of opioids via intermittent bolus, continuous infusion, or combinations, without any influence on the continuous infusion of a secondary non-opioid medication. This may also reduce side effects because it uses the lowest possible doses of each drug, preventing development of tolerance and hyperalgesia. As presented in Section 3, recent developments in micromachined components have enabled a two-valve manifold with multiple embedded pressure sensors to regulate flow from multiple pressurized reservoirs, preserving the high-VER and low-power benefits of the valve regulated architecture.

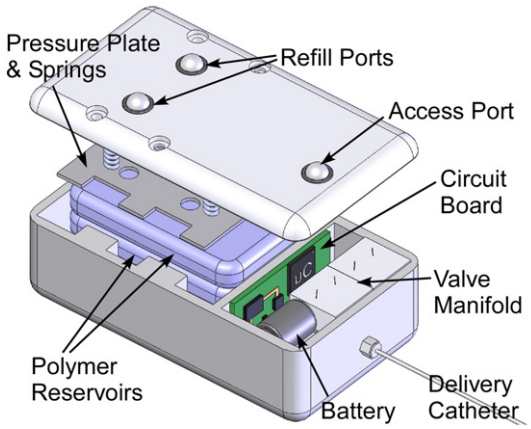

Fig. 1. Concept of the valve-regulated drug delivery system. Dual-drug delivery is illustrated as example: drug reservoirs are pressurized by springs; drug delivery is regulated by MEMS valves with embedded pressure sensors. On-board control electronics allow pressure monitoring and re-programming.

2.2. Insulin pump

External, wearable drug pumps have been in common use for automated insulin infusion in diabetes therapy [51]. Many commercial products have been developed, such as MiniMed Paradigm® Revel™ from Medtronic [52], OneTouch® Ping® from Animas [53], OmniPod® from Insulet [54], Dana Diabecare® from Sooil [55], Deltec Cozmo® from Smiths Medical [56], ACCU-CHEK® Spirit from Roche [57], and

Table 1
Comparison of current commercial intrathecal implantable pumps [44–47].

	SynchroMed EL	SynchroMed II	IsoMed	CODMAN 3000
Manufacturer	Medtronic	Medtronic	Medtronic	Codman
Volume (cm^3)	123.1, 156.8	117.3, 156.4	111.8, 135.0, 172.3	94, 219.3
Weight (empty)	185, 205 g	165, 175 g	113, 116, 120 g	98, 173
Reservoir size	10, 18 mL	20, 40 mL	20, 35, 60 mL	16, 50 mL
Battery life	≈5.5 years at 0.9 mL/day	7 years at 0.9 mL/day	No battery	No battery
Flow rate (mL/day)	0.048–0.9 (programmable)	0.048–24 (programmable)	0.3, 0.5, 1.0, 1.5, 4.0 (constant flow)	0.3, 0.5, 1.0, 1.3, 1.7, 3.4 (constant flow)

Zone® from Spring (formerly NiliMEDIX) [58]. The majority of these pumps use a motorized peristaltic or rotary pump to deliver the medication [52–57]. In most pumps insulin is delivered through a tube that is connected to a disposable cannula. One exception is the OmniPad®, for which a hidden needle is automatically inserted as needed [54]. In all insulin pumps, both basal and bolus deliveries can be provided according to a programmed schedule. These external pumps provide less battery life and smaller reservoirs than current intrathecal pumps of a similar size. The infusion set (tubing and cannula) is replaced every 2–3 days, and the battery is an AA or AAA replaceable one that lasts for a few weeks. Although insulin pumps are used as wearable devices instead of implants and thus size is not a major concern, the relatively large form factor is still an issue for comfort and convenience in everyday use. This is even more significant for pediatric patients. The motor used for fluid driving can compromise the volume that is otherwise available for the drug reservoir, reducing both volume and power efficiency.

An alternative approach uses valves to regulate flow from a pressurized reservoir, similar to that discussed in Section 2.1 for intrathecal applications. This has been demonstrated in the Spring Zone® insulin pump, which claims to be the smallest insulin pump with tubing currently on the market [58]. The durable, reusable portion of the device includes valve actuators, temperature and pressure sensors, control electronics and user interface, battery and housing. The disposable cartridge includes a spring-pressurized reservoir, mechanical valves and other flow control components, and an infusion set. By eliminating the motor and placing most moveable parts in the disposable cartridge, higher reliability and volume efficiency of the pump are promised. The valve is electronically modulated to compensate for the change in delivery rate as the reservoir gradually deflates, resulting in high-precision, constantly-monitored, insulin delivery. This is especially important for patients with high insulin sensitivity, e.g. Type 1 diabetes patients with renal failure and children. As discussed in Section 2.1, by using micromachined components and monolithic integration of valves and sensors, devices can be further improved for a smaller form factor, higher volume and power efficiency. Multi-drug delivery from one integrated device can also be facilitated.

As mentioned in Section 1.2, delivery of multiple hormones, such as insulin, glucagon, and amylin, is greatly desirable in diabetes therapy. Currently, integrated pumps that can deliver two or more hormones, which are referred to as artificial pancreas in some cases, are still under development [59,60]. Patients who use glucagon or amylin inject them daily, either by a syringe or a separate insulin pump. These hormones cannot be mixed and loaded into a single reservoir. Hence, a valve-regulated pump with multiple reservoirs for individual hormones presents an attractive solution. The high volume efficiency enabled by micromachined and monolithically-integrated components is also an asset.

3. An architecture based on microsystems technology

As noted in Section 2, a valve-regulated system architecture for drug delivery provides a number of benefits that could improve target medical therapies, such as intrathecal drug delivery and insulin delivery [48,61]. Shown in Fig. 1 is an implementation for dual-drug delivery to demonstrate these benefits. The three major components of this system are the microvalve with embedded microsensors, the pressurized reservoir, and the control and communication circuitry.

3.1. Microvalve with embedded microsensors

The throttling microvalves should be able to regulate flow at rates necessary for the delivery of target drugs. The valves must additionally withstand reservoir pressures, have a small form factor, and be energy efficient. To accommodate multi-drug delivery, the valve design should also be scaled for use in manifolds.

An active valve with embedded pressure sensors can be used to servo-control the flow rate and the total delivered volume from the reservoir. The reservoir pressure, which, in this architecture, provides the mechanical force for the drug delivery, diminishes as the reservoir is depleted (i.e. the pressure decreases as a function of the residual volume). A pressure sensor embedded at the inlet of a throttling microvalve can be used to monitor this pressure, thus providing a measure of the residual volume in the reservoir. Monitoring the volume changes over time provides one approach to determine the flow rate. Alternatively, the differential pressure across a microvalve can be directly obtained from the readings of the pressure sensors embedded at the inlet and outlet of the valve. The flow rate can then be derived from this differential pressure and the given flow resistance of the valve. Both methods of flow rate monitoring can be implemented simultaneously to provide redundancy and eliminate potential dosing errors. Using measured data on the flow rate, control algorithms programmed in a μC can then be used to modulate the valve for a target flow rate.

Active microvalves generally include a variable flow channel that is modulated by an actuator. Although actuation mechanisms used in microvalves range from electrostatic to thermal phase-change [62–71], a piezoelectric approach is favorable because it consumes low power and generates forces that allow valve operation across a wide range of operating pressures.

As shown in Fig. 2, the microvalve operates by pressing a serpentine valve seat against a glass wafer using a piezoelectric actuator. A silicon-on-insulator (SOI) wafer is used as the device substrate to ease the co-fabrication with embedded sensors. A membrane with a serpentine valve seat is formed on the top side, which is the Si or substrate side of an SOI wafer. The valve seat is located on a central boss that also houses a pressure sensor and presses against a glass plate with an inlet and an outlet. The elongated valve seat provided by the serpentine geometry increases the flow perimeter which compensates for the limited deflection of the piezoelectric actuators and enables modulation of larger flow rates [72]. The piezoelectric actuator can be a commercially-available lead zirconate titanate (PZT) stack such as those from Physik Instrumente, Germany. The spacing between the valve seat and the glass plate is 0–2 μm. This creates a channel with a much higher hydraulic resistance than the delivery catheter, allowing accurate flow regulation in the range of interest. The back side, which is the epitaxial side of the SOI, has boron doping and gold traces for electrical connections to the pressure sensors.

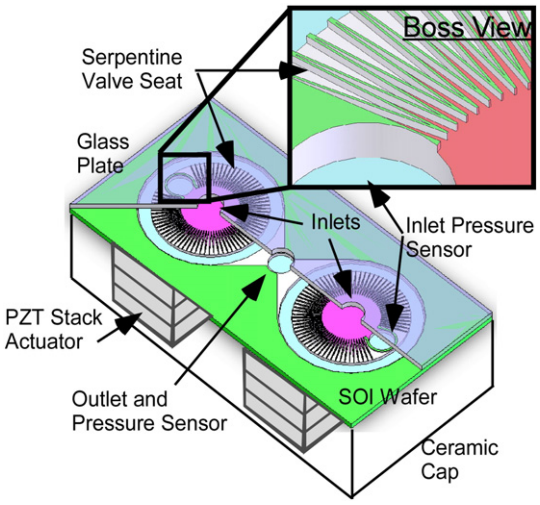

Fig. 2. Concept schematic of a dual-valve manifold.

The design of the single microvalve can be easily scaled toward a valve manifold with multiple seats. Fig. 2 shows a valve manifold with two seats used to regulate flows from two inlets. Each inlet uses its own pressure sensor to independently monitor the input pressure from the corresponding reservoir. The manifold has a common outlet with a single outlet pressure sensor for mixing in the device and common flow control. The small size and low-power consumption of the valve manifold allow for multiple drug reservoirs and smaller batteries to be used without increasing the size of the drug delivery system.

The embedded pressure sensor can be either piezoresistive or capacitive. Piezoresistive sensors made from implanted silicon are chosen; Wheatstone bridges are used for readout of the sensors because these are easy to interface with and have lower output impedance than capacitive readouts. A target sensitivity of >600 ppm/kPa is desired for an accurate feedback control.

The microvalve or valve manifold with embedded pressure sensors can be fabricated from an SOI wafer and a Pyrex glass wafer using standard micromachining technologies for micro electromechanical systems (MEMS). The details of one fabrication process are provided in [61]. The valve plates can be individually adjusted during fabrication to create a normally-open, a partially-open, or a normally-closed valve [73]. For intrathecal pumps, a partially-open valve is favored for fail-safe operation. The fabricated valve plates are assembled with the PZT actuator stacks inside a customized Macor® ceramic housing. Fig. 3 shows a fabricated dual-valve manifold. Fig. 4 presents test results from the dual-valve operation. For this test, liquid was injected at 14 kPa to individual or both valves (i.e. Valves A, B, or A and B). With an 80 V actuation voltage range, the flow rate varied from 1.77 to 0.028 mL/h through Valve A, and from 2.12 to 0.38 mL/h through Valve B, when each valve was open individually. When both valves were open together, flow rates combined from each valve in two separate regimes. At high flow rates (>2 mL/h), the catheter resistance dominated the flow and valve modulation was less effective. At lower flow rates (<2 mL/h), valve resistance dominated, and the combined flow rates were close to the sum of the individual flow rates through each valve. The embedded pressure sensors showed a sensitivity of 698 ppm/kPa at room temperature, exceeding the design target [61].

Compatibility with magnetic resonance imaging (MRI) is generally a concern for conventional motor-driven implanted pumps due to the strong magnetic fields present during the diagnostic procedure. Although not assessed, it is notable that the microvalve discussed here does not use any material that is susceptible to strong magnetic fields, suggesting that it is naturally more accommodating to MRI conditions.

3.2. Pressurized reservoir

Many methods have been utilized for pressurizing reservoirs in drug delivery systems, including those using pressurized gas, mechanical springs, material elasticity, or osmotic pressure gradients. Depending on the specific approach used for implementation, the pressurizing mechanism can consume a significant volume when compared to the volume used for the fluid itself, diminishing the VER of the overall system. Besides VER, factors of significant importance in the design of a pressurized reservoir include the pressure–volume relationship (PVR) and the dead volume. The PVR refers to the relationship between the liquid pressure in the reservoir and the volume remaining in the reservoir. A certain amount of the stored liquid cannot be delivered when the pressure in the reservoir drops too low. The dead volume includes this undeliverable volume as well as the volume of the reservoir that is not liquid.

One possible implementation of pressurized reservoirs for dual-drug delivery is shown in Fig. 5 [61]. In this, two compliant reservoirs made from a material such as polyethylene are stacked in a metal housing and pressurized through compression by a metal plate. The reservoirs have an inlet tube from a refill port on the housing, as well as an exit tubing to the valve manifold and its inlet pressure sensors. The compressed springs push the pressure plate against the top reservoir in the stack, which, in turn, presses the bottom reservoir. Vertical guides in the plate and in the casing maintain alignment of the plate, springs, and reservoirs during assembly and compression. The pressure response of the reservoir can be adapted to specific system needs by appropriately designing the compressive springs; e.g., different delivery pressures are needed for intrathecal drug delivery and subcutaneous insulin delivery. The energy stored in the spring is dissipated while liquid in the reservoir is being delivered,

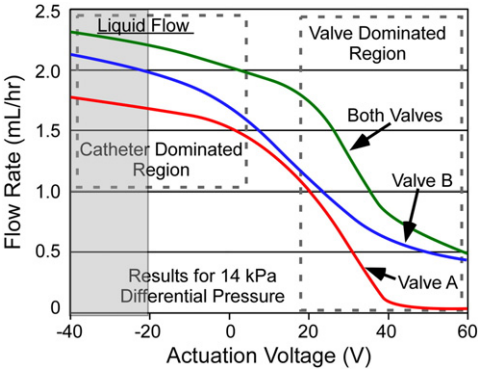

Fig. 4. Flow rate of alcohol through individual and combined valves in a manifold at 14 kPa. Catheter resistance is greater than the valve resistance at low voltages outside the preferred operating region. This results in reduced modulation. Mixing also functions as expected, and is particularly evident in the lower flow rate regimes.

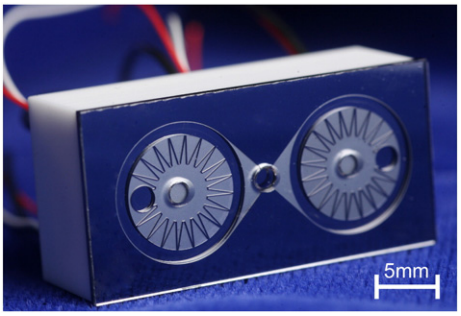

Fig. 3. Photograph of an assembled dual-valve manifold for multi-drug protocols. Both serpentine valve seats are clearly visible and the common outlet port is located in the center of the die. The manifold measures 3×1.5×1.1 cm^3 [61].

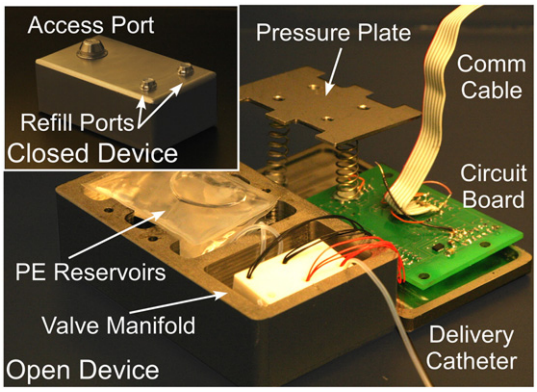

Fig. 5. A prototype of a dual-drug delivery system pictured during assembly. Two polymer reservoirs are pressurized using a spring-loaded plate. Flow is monitored and regulated by a PZT-actuated valve manifold with embedded pressure sensors. The entire system takes up about 130 cm^3. The inset shows a photograph of the closed system with the refill and catheter access ports [61].

and is recharged when the reservoir is refilled. An appropriate stiffness for the spring-loaded reservoir is in the range of 0.1–10 kPa/mL.

For reservoirs with a repeatable PVR in which the reservoir generates decreasing pressure with decreasing volume, such as the one shown in Fig. 5, microsensors integrated with the reservoir or the inlet of the regulatory valve can be used to indirectly measure the residual drug volume by measuring the pressure. Reservoirs with this type of PVR can realize volume efficiencies >80%. Feedback control is required for a varying pressure reservoir to account for pressure variations and achieve accurate dosing. This can be implemented using the same set of pressure sensors.

The architecture reported in [48] used three ports for intrathecal drug delivery. Two of these ports are standard refill ports (Instech Laboratories, Plymouth Meeting, PA; model MIC) that are integrated into the system casing and connected to the two reservoirs by tubing. These ports permit the reservoirs to be filled by a syringe equipped with a Huber needle. They can be modified as discussed in Section 5 to enable transdermal power delivery. The third port is a fluidic access port. The port is routed directly to the catheter so that a physician can circumvent the device for direct access to the CSF. In contrast, a replaceable infusion set is used for insulin delivery, eliminating the need for ports.

3.3. Control circuitry and power

A number of functions must be implemented by control electronics. For example, the input from the pressure sensor must be amplified and read into a μC. The data from the pressure sensor must be processed and, together with the target delivery rate information, used in control algorithms. The valve actuation voltage necessary for the desired flow must be generated by a charge pump amplifier circuit. Minimally, the control system must efficiently accommodate multiple sensor inputs, storage of complex delivery programs, and the capacity to drive the valves across operating voltages.

Because the piezoelectric valve consumes power primarily during transitions of its set point, the primary source of power consumption in a valve-regulated drug pump is the electronic control and communication system. A low-power μC with embedded memory should be used to control the valves, process the sensor data, and perform high-level tasks of communication. It should also specify to the power management circuit elements when devices should be put into sleep mode, or awoken. The power electronics consisting of battery regulators and power amplifiers should be able to power everything from the sensors to the valves. This is a wide range of output voltages (typically from 2.5 V to 75 V). The converters for these voltages must be as efficient as possible, and still run off a single battery. Alternatively, a battery recharging circuit can be included to recharge the battery during the refill sessions for implanted applications. This relaxes power constraints on the control circuitry. More details of the transdermal power delivery scheme are provided in Section 5.

A prototype control circuit (Fig. 6) designed to enable feedback from the embedded sensors to operate the system has been reported recently [48]. The circuit was operated from a battery providing 3–4 V. The battery regulator (LT 1761 from Linear Technologies) was selected for power efficiency. The selected μC was MSP430F169 from Texas Instruments (TI). It was well suited to this application because it had the necessary peripherals (ADC and DAC), a low-power sleep mode in which it consumes 2 μW, and a power consumption of 600 μW when active. Capacitive boost–boost amplifiers (LT3482 from Linear Technologies) were used to amplify the output signals from the microprocessor to power the piezoelectric actuators in the valves. The differential input from the Wheatstone bridge with piezoresistive pressure sensors was amplified and converted to a single-ended output voltage by AD623 (Analog Devices) instrumentation amplifiers. These amplifiers were shut down when not reading pressure, greatly reducing the power draw. This circuit board was a double-sided, two-metal-layer board that measures $4 \times 6\ cm^2$.

Different control algorithms can be implemented. Given the flow information obtained by the embedded pressure sensors, continuous drug delivery can be regulated by slowly adjusting the aperture of the valve to compensate for the decreasing reservoir pressure as delivery proceeds. Alternatively, a binary duty cycle control can be used for regulation, in which the valve is either open or closed [48]. This can be used as an effective approach to overcome the hysteresis in the piezoelectrically-operated valves. The duty-cycle regulation still appears continuous to the patient at the catheter/CSF interface because the fluidic capacitance of the catheter can average the delivery profile. In addition, a bolus dose can be delivered by fully opening the valve

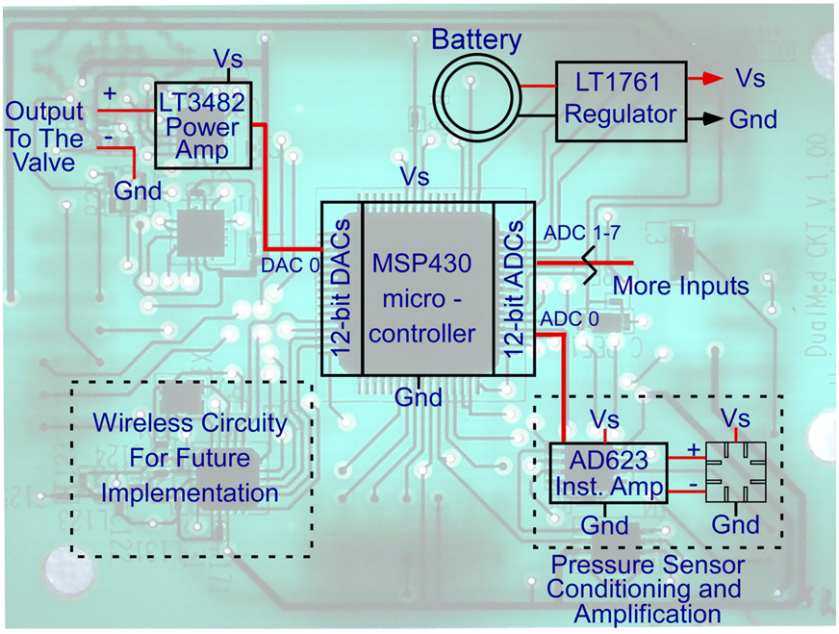

Fig. 6. A preliminary version of the control circuit (without wireless capability) built on a PCB of $4 \times 6\ cm^2$ area and powered by a 3 V battery [48].

until the desired volume is delivered. These continuous and bolus control algorithms can be combined to realize unique delivery profiles or respond to environmental stimuli.

The intrinsic hysteresis of the piezoelectric actuator can cause error in flow rate regulation if it is not accounted for. If continuous flow regulation is the only technique employed, hysteresis can be accounted for by following one side of the hysteresis curve due to the fact that the valve is gradually opened and never closed until the reservoir is refilled. Alternatively, the duty-cycle regulation can provide a more accurate means of control [48]. If bolus or mixed regulation methods are employed, the hysteresis must be calibrated to establish an internal control model that accounts for increasing or decreasing actuation voltage.

The implementation of the control algorithms and other circuit functions will dominate the power consumption of the device, but there are compromises between power consumption and delivery accuracy that can be used to reduce the battery drain. More details of these control algorithms and their relationship with power consumption of the valves can be found in [48,49]. The worst-case power consumption of the valve for any possible operation was determined to be 1.6 μW.

In a servo-controlled architecture that measures the actual flow rate achieved by the drug delivery device, significant error can result from an inaccurate measurement of the flow rate. In the valve-regulated architecture, the flow rate will be calculated by the control electronics by a sequence of pressure readings. Compensation for temperature variations and non-linearities associated with operating pressures and flow rates can be easily determined during the initial calibration and stored in the onboard memory of the μC, either in a look-up table or as polynomial coefficients. It is, however, worthwhile to estimate the resolution in the pressure readings, because these factors cannot be compensated.

The pressure of the reservoir is linearly related to the flow rate through the reservoir; it is estimated that all desirable flow rates can be achieved for residual pressures >500 Pa. The maximum error in delivery due to sensor properties will occur at the lowest delivery pressure. For the system described in [61], it is estimated that this is 500 Pa. For the flow rate error to remain <2.5% of the delivery rate, the minimum resolvable pressure difference for the sensors must be 12.5 Pa. In the prototype system that uses a 12-bit analog to digital converter (ADC) with the piezoresistive pressure sensors, the electronics is able to resolve a pressure difference of 4.88 Pa [48].

Typically, intrathecal CSF pressure varies from 0.7 kPa to 1.8 kPa in healthy adults [74]. Fig. 7(a) shows example measured flow rates with compensation for variations in delivery pressure, with comparison to uncompensated flow rates [61]. In this particular case, the uncompensated flow rates decreased from 0.58 mL/h to 0.21 mL/h as the delivery load pressure was increased. In contrast, the flow compensation program adjusted the valve actuation voltage and maintained a flow rate of 0.58 mL/h within a 0.5% range.

In controlled flow tests, both reservoirs were pressurized by the spring driven plate and filled via the refill ports. These were then used for delivery through the valve manifold. The manifold was driven by a 0–60 V square wave running at 0.02 Hz; the duty cycle of this signal was varied to modulate the flow rate. Fig. 7(b) shows the results of a typical test. Three target flow rates were programmed during a 200 minute period. The instantaneous deviation of the measured flow rates from the targets was no more than 0.01 mL/h. All measured flow rates were well within medical limits of less than 15% deviation from the target delivery rate [75].

Using a single valve system [48], third order polynomial models of the flow rate were investigated for calibration and non-linearity compensation for the embedded sensors and the valve. These models were incorporated into a microprocessor program to regulate continuous flow. Flow measurements typically extended from several hours to a week. One typical test (Fig. 8a) demonstrated

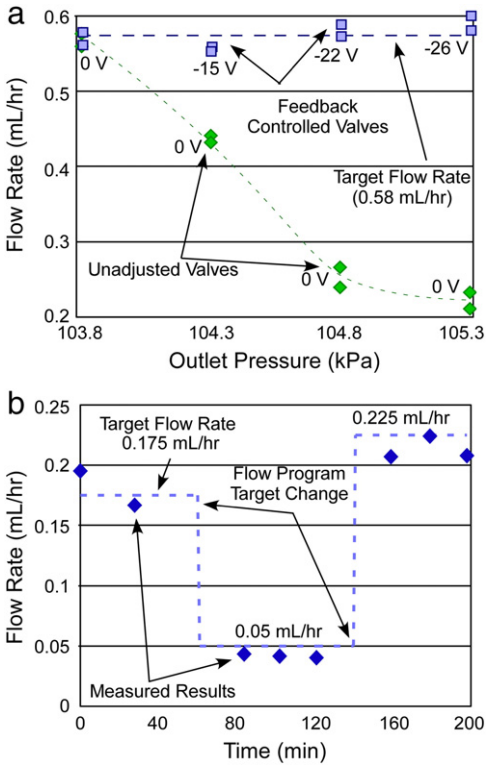

Fig. 7. (a) Flow and actuation voltages for varying delivery pressures to represent unregulated and regulated flows using the internal pressure sensor at the valve outlet. Unregulated flow varied from 0.58 mL/h to 0.21 mL/h while regulated flow remained within 0.5% of the target flow rate. (b) A typical result of duty cycle regulation of flow through the manifold with multiple set points. In this instance, the duty cycle of a 60 V square wave at 0.02 Hz is altered to achieve a mixed flow at the target delivery rates [61].

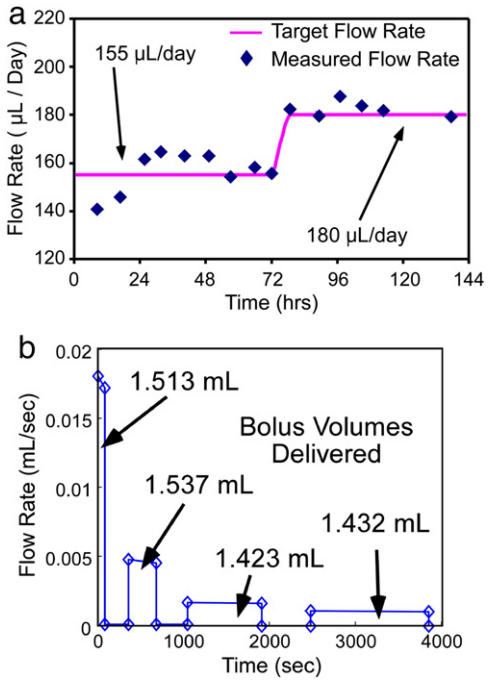

Fig. 8. (a) Preliminary exploration of steady-state flow: 155 μL/day for 3 days followed by 180 μL/day for the next 3 days. The flow rates for each set-point have a maximum deviation from the target flow rate of 9.09% and an average deviation of 3.22%. The total volume delivered was within 0.39% of the target volume for the time period. (b) Preliminary results for bolus delivery. The total volume delivered in four equal doses was 5.971 mL [48].

average delivery accuracies of 3.22% with no instantaneous deviation from the flow rate worse than 9.09% at delivery rates of <0.2 mL/day. Under laboratory conditions, the total delivered volume over the 6-day period was within 0.39% of the target volume. Bolus delivery was also demonstrated with a microvalve and reservoir model using a calibrated pressure–volume relationship. A program was built to deliver a total volume of 6 mL in four 1.5 mL bolus doses (Fig. 8b). The valves were actuated based on a predetermined pressure–volume relationship of the reservoir. These results suggest that high accuracies can be achieved using the valve-regulated architecture for drug delivery.

3.4. Failure mode testing

The most common failure modes encountered in drug delivery with conventional pumps are catheter-related problems, such as dislodgement, dislocation, kink/occlusion, or disconnection of catheters. Problems with the pumps are rare and may include premature end-of-life and sometimes inability to deliver the set amounts of drug.

Conventionally, the first indications of a fault in drug delivery are symptoms related to alterations in medication rates. If the patient unexpectedly receives no analgesic benefit, an occluded or disconnected catheter may be indicated. The resulting withdrawal can be life threatening in some cases, such as when the medication being delivered is Baclofen for treating spasticity. One of several techniques may then be used by physicians to determine the actual alterations in the catheters, such as tracing radioactive dye through the delivery chain and surgical investigation.

In the valve-regulated systems, the embedded pressure sensors on the microvalves can allow the system to detect these conditions before a patient experiences discomfort or acute withdrawal. The response of embedded pressure sensors to catheter kinks was described in [61]. In a bench-top test, the tip of the catheter was blocked for varying durations of time (Fig. 9a). The test showed an increasing pressure ramp associated with the blockage; this pressure ramp was repeatable and steeper than any others that may occur during normal operation. The embedded pressure sensors, therefore, can be used to detect an occluded catheter within several seconds.

The response of the pressure sensors for catheter disconnects was tested in a similar manner (Fig. 9b). A significant initial drop in the pump outlet pressure was observed at the time of the disconnection. The pressure then settled to a new value. Although the in vivo pressure change is likely to have a lower magnitude, a rapid drop in the outlet pressure will potentially signify acute disconnects.

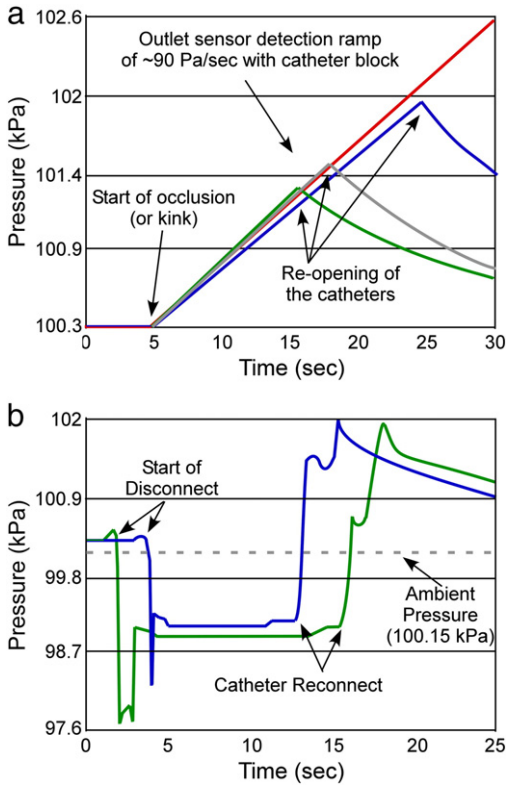

Fig. 9. (a) Outlet pressure before, during, and after the catheter is blocked. The sensor detects a pressure ramp of about 90 Pa/s when the catheter is occluded. (b) Oscilloscope traces of the outlet pressure sensor when the catheter is acutely disconnected and later reattached to the drug delivery device. The tests were conducted in ambient air; some artifacts of the sensor response may be due to test conditions [61].

4. Other sensors for integration

In addition to pressure sensors, a number of other sensors are of interest for integration with the valve-regulated drug delivery system. Incorporation of a glucose sensor into the overall control loop is particularly attractive for insulin pumps.

Effective control of hyperglycemia with insulin relies on accurate monitoring of the blood glucose level and corresponding adjustment of insulin delivery rate. Traditional finger-prick measurements of blood glucose often miss hypoglycemic and hyperglycemic events occurring through the day because glucose levels can change rapidly. Nocturnal hypoglycemia, which a patient experiences during sleep, often goes undetected and may have severe consequences including seizures and brain damage. Improved detection of nocturnal hypoglycemia and moderate improvement in glucose control and reduction in hypoglycemia with a sensor-augmented insulin pump in an open system and a closed-loop system have been well documented [76–78]. In such a system a sensor is used to continuously monitor interstitial glucose levels, which are then used by the physician and patient to alter the insulin delivery rate. Current insulin pumps and glucose sensors in the market are not operated in closed-loop and the development of control algorithms to guide this process is being actively pursued and investigated.

There are challenges in the science and technology for both sensors and control algorithms. Designing continuous glucose monitoring systems (CGMS) has been a research focus for years and continues to remain the target of extensive research. These sensors have been widely explored for miniaturized and portable systems [79–87]. Currently available commercial products are mostly based on enzymatic subcutaneous electrodes, such as Paradigm® (Medtronic Diabetes, Northridge, CA, USA), DexCom STS® (Dexcom, San Diego, CA, USA), and Abbott FreeStyle® Navigator (Abbott Diabetes, Alameda, CA, USA). However, repeatability, reproducibility, and long-term stability of such sensors can be challenging to achieve because the sensitivity depends upon the activity of immobilized enzymes [88–90]. Non-enzymatic and non-invasive glucose detections under development use optical and transdermal modalities such as mid-infrared and near infrared spectroscopy, optical coherence tomography, sonophoresis, photoacoustic spectroscopy, fluorescence, etc. Among these, a technology that can be potentially integrated with an insulin pump uses an electrode with active bioreceptor. This bioreceptor can be modified by nanomaterials to provide affinity for a particular biomolecule and reject others. In early demonstrations, TiO_2 nanotube arrays decorated with CuO nanoparticles have shown promising results [91–93].

5. Transdermal power delivery

Conventional implantable active drug pumps, such as those for intrathecal delivery, typically have a significant battery size that can be 25–50% of the total device volume in order to sustain continuous operation over the implant lifetime (5–10 years). Replacing this traditional battery with a smaller rechargeable battery can improve the

VER of the implant substantially or alternatively reduce the device size by up to 40%, providing efficiency and convenience. This is particularly true for devices that have long implant lifetimes and relatively high rates of power consumption like the intrathecal drug pumps [94]. The recharging capability also allows greater system versatility because more energy intensive functions can be implemented.

A number of approaches can be used to charge implantable batteries. Wireless power transfer using a wireless radio frequency (RF) link or a wireless inductive link is better suited for very low-power applications [95]. Instead, DC recharge with a direct physical connection offers higher current levels and may be more suitable for implantable drug delivery devices [96]. The only direct connection between the implanted drug pump and the external environment occurs when a needle is inserted into the subcutaneous refill port for reservoir refill. These refill ports are inset within the wall of the pump housing [97]. The ports typically consist of a biocompatible shell, a resealable silicone septum, a metal base plate to limit needle penetration depth, and a cavity between the septum and the base plate with an exit channel through which the fluid reaches the reservoir [98,99]. In a typical refill session, a non-coring Huber needle is inserted to puncture the septum until the needle tip presses against the base plate. Medication is then driven from an external syringe through the needle into the pump reservoir [100]. This process generally takes 10–20 min and occurs every 8–12 weeks.

To achieve transfer of electrical power to implantable drug pumps, a customized bifurcated needle has been reported (Fig. 10) [101]. This approach is intended for rapidly charging implant batteries with enough power to replace what is used between refill visits. The needle for recharging consists of two halves of a 26 gauge (0.46 mm outer diameter) stainless steel Huber needle that is split longitudinally. This allows two isolated conductive pathways when the two halves are bonded together to form a complete needle [102]. Selective coating of the surfaces of the needle halves with Parylene provides electrical isolation between the two pathways. A 50 μm-thick Kapton tube wrapped outside the bonded needle provides further insulation and sealing strength. The septum of the refill port includes two micromachined stainless steel contact springs and self-healing polydimethylsiloxane (PDMS) supporting layers. The contact springs mate electrically with the modified needle when the needle is fully inserted into the refill port. The mating is designed to be self-aligned regardless of the rotational orientation or insertion angle of the needle. This avoids the need for the physician to rotate or reinsert the needle for proper contact, which may result in additional risk of infection and patient discomfort beyond those already experienced in the refill process [42].

Experiments have demonstrated effectiveness of the electrical contact and insulation of the charging needle and refill port in both wet and dry ambient environments. The average contact resistance between the needle and the port is $<2\ \Omega$ in either environment. Preliminary verification of mechanical reliability and longevity of the refill port is provided by repeated needle insertions for 100 times, and $\approx 1\ \Omega$ variation in contact resistance is exhibited. The results suggest that this power delivery method can be used to enable battery recharging for an implant.

6. Conclusions and future prospects

A microvalve-regulated architecture that can offer high performance and volume efficiency has been demonstrated. Current research in microsystems technology indicates that piezoelectric microvalves with embedded pressure sensors can be used to actively regulate dosing by throttling flow from a mechanically-pressurized reservoir. Specific un-powered flow rates can be set by assembling the throttle valves with a nominal gap that meets the delivery needs. This can be used to create a fail-safe delivery (in cases of power loss) that can prevent hazardous withdrawal or overdose effects. The potential for administering multi-drug protocols has been demonstrated by using a dual-valve manifold to modulate and mix drug flows from two separate reservoirs. In one of the prototype systems for dual-drug protocol, the valve manifold, reservoirs, control and power electronics, and access ports are integrated in a metal casing with a total volume of 130 cm^3. Several control modes have been evaluated to mimic clinical applications, including drug delivery in bolus flow, continuous flow and a combination of both. Bolus units were delivered with a total error of 0.48%. The flow rates of bolus and continuous flow deliveries ranged from 2.30 mL/h to 0.51 mL/h. Larger and smaller rates can both be achieved by adjusting the design parameters of the valves or reservoir springs. In six-day tests performed at low flow rates (0.1–0.2 mL/day), delivery was regulated with average accuracies of 3.22% and a total delivered volume within 0.4% of the target. Additional tests demonstrated the capability to compensate for changes in delivery pressure, such as the spinal fluid pressure for intrathecal application, and subcutaneous pressure for insulin delivery. The measured pressure profiles can also be used

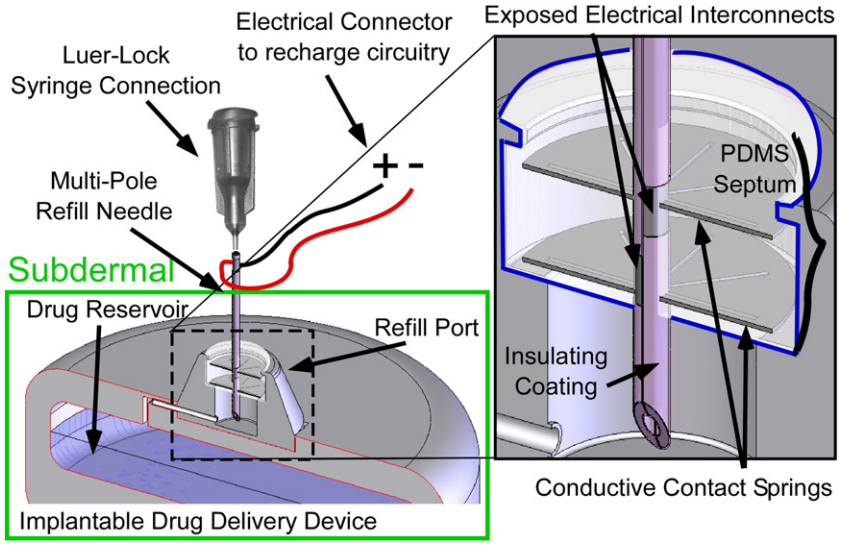

Fig. 10. Schematic for transdermal power delivery using MEMS technology. A two-pole needle is inserted into the refill port of a drug delivery device. Inset: a close view of the two needle halves making electrical contact with springs inside the septum [101].

to detect catheter occlusions and disconnects. The piezoelectrically-actuated valve manifold showed no measureable sensitivity to moderate magnetic fields; further tests are needed to fully characterize the impact of MRI-strength magnetic fields on the valve operation.

Drug delivery systems using this architecture can be scaled up or down in size for many applications, such as the delivery of antibiotics, cancer chemotherapeutic agents, and hormone therapy in a variety of medical conditions. The reservoir size, shape, or the valve modulation range can be adapted for each application. Further miniaturization of system components and optimization of the assembly process can help reach a VER of over 60%. Additional sensors that measure other physical properties can be embedded with the valves to expand the information available to the clinician, or to further improve the accuracy and the safety of the device. A wireless communication protocol, such as Bluetooth, can also be implemented for interaction with external systems and other implants. This can provide the interface for a clinician to receive statistical data of the system and reprogram the delivery schedule that best suits the patients' need.

In the long term, the ultimate goal of insulin delivery is a closed-loop system in the form of an artificial pancreas. It can monitor the glucose level and accordingly adjust the delivery of multiple hormones. This is important for Type 1 diabetes, hospitalized patients with diabetes and eventually Type 2 diabetes. Insulin sensing and insulin delivery have significant variability not only between individuals, but also for a single individual, which contributes to the complexity of the control algorithm used in the closed-loop system. Mimicking the pancreatic beta cell transplant has been considered and a silicon beta cell which has the ability to provide basal insulin and bursts of prandial or meal insulin has recently been described [103,104]. Integrating this with a sensor may be an emerging technology for the future [105].

Acknowledgment

The authors gratefully acknowledge Dr. Jong Moon Park for early contributions to the microvalve development. The research effort was supported, in part, by a grant from the University of Michigan, Department of Internal Medicine, Division of Anesthesiology, and a grant from the Michigan Institute for Clinical and Health Research (MICHR). Facilities used for this research include the Lurie Nanofabrication Facility (LNF) operated by the Solid-State Electronics Laboratory (SSEL) at the University of Michigan.

References

[1] Joint Committee on Accreditation of Healthcare Organizations, New standards to assess and manage pain, Jt. Comm. Perspect. 19 (1999).
[2] C.J. Phillips, Pain management: health economics and quality of life considerations, Drugs 63 (2003).
[3] C. Harstall, M. Ospina, How prevalent is chronic pain? Pain: Clinical Updates, Online Newsletter of International Association for the Study of Pain, Jun. 2003 http://www.iasp-pain.org.
[4] N.G. Rainov, V. Heidecke, Management of chronic back and leg pain by intrathecal drug delivery, Acta Neurochir. Suppl. 97 (2007).
[5] J.A. Turner, J.M. Sears, J.D. Loeser, Programmable intrathecal opioid delivery systems for chronic noncancer pain: a systematic review of effectiveness and complications, Clin. J. Pain 23 (2007) 180–195.
[6] E.S. Krames, K. Olson, Clinical realities and economic considerations: patient selection in intrathecal therapy, J. Pain Symptom Manage. 14 (1997) S3–S13.
[7] M. Winkelmuller, W. Winkelmuller, Long-term effects of continuous intrathecal opioid treatment in chronic pain of nonmalignant etiology, J. Neurosurg. 85 (1996) 458–467.
[8] D.P. Wermeling, Ziconotide an intrathecally administered N-type calcium channel antagonist for the treatment of chronic pain, Pharmacotherapy 25 (2005) 1084–1094.
[9] S.A. Schug, D. Saunders, I. Kurowski, M.J. Paech, Neuraxial drug administration: a review of treatment options for anaesthesia and analgesia, CNS Drugs 20 (2006).
[10] R.L. Rauck, D. Cherry, M.F. Boyer, P. Kosek, J. Dunn, K. Alo, Long-term intrathecal opioid therapy with a patient-activated, implanted delivery system for the treatment of refractory cancer pain, J. Pain 4 (2003).
[11] T. Deer, I. Chapple, A. Classen, K. Javery, V. Stoker, L. Tonder, K. Burchiel, Intrathecal drug delivery for treatment of chronic low back pain: report from the National Outcomes Registry for Low Back Pain, Pain Med. 5 (2004).
[12] S. Erdine, J.D. Andres, Drug delivery systems, Pain Pract. 6 (2006).
[13] R. Likar, W. Ilias, H. Kloimstein, A. Kofler, H.G. Kress, J. Neuhold, M.M. Pinter, M.C. Spendel, Importance of intrathecal pain therapy, Der Schmerz, 21 (2007) 15–27.
[14] E.S. Krames, Intraspinal opioid therapy for chronic nonmalignant pain: current practice and clinical guidelines, J. Pain Symptom Manage. 11 (1996) 333–352.
[15] T.J. Lamer, Treatment of cancer-related pain: when orally administered medications fail, Mayo Clin. Proc. 69 (1994) 473–480.
[16] J.S. Crawford, Site of action of intrathecal morphine, Br. Med. J. 281 (1980).
[17] A. Baraka, Rostral spread of intrathecal morphine in man, Middle East J. Anaesthesiol. 6 (1982).
[18] I. Dobrydnjov, K. Axelsson, A. Gupta, A. Lundin, B. Holmström, B. Granath, Improved analgesia with clonidine when added to local anesthetic during combined spinal–epidural anesthesia for hip arthroplasty: a double-blind, randomized and placebo-controlled study, Acta Anaesthesiol. Scand. 49 (2005) 538–545.
[19] S. Strebel, J.A. Gurzeler, M.C. Schneider, A. Aeschbach, C.H. Kindler, Small-dose intrathecal clonidine and isobaric bupivacaine for orthopedic surgery: a dose–response study, Anesth. Analg. 99 (2004) 1231–1238.
[20] L.L. Ackerman, K.A. Follett, R.W. Rosenquist, Long-term outcomes during treatment of chronic pain with intrathecal clonidine or clonidine/opioid combinations, J. Pain Symptom Manage. 26 (2003) 668–677.
[21] N.G. Rainov, V. Heidecke, W. Burkert, Long-term intrathecal infusion of drug combinations for chronic back and leg pain, J. Pain Symptom Manage. 22 (2001) 862–871.
[22] T.R. Deer, D.L. Caraway, C.K. Kim, C.D. Dempsey, C.D. Stewart, K.F. McNeil, Clinical experience with intrathecal bupivacaine in combination with opioid for the treatment of chronic pain related to failed back surgery syndrome and metastatic cancer pain of the spine, Spine J. 2 (2002).
[23] E.I. Uhle, R. Becker, S. Gatscher, H. Bertalanffy, Continuous intrathecal clonidine administration for the treatment of neuropathic pain, Stereotact. Funct. Neurosurg. 75 (2000) 167–175.
[24] M.S. Wallace, R. Rauck, R. Fisher, S.G. Charapata, D. Ellis, S. Dissanayake, Z.-S. Group, Intrathecal ziconotide for severe chronic pain: safety and tolerability results of an open-label, long-term trial, Anesth. Analg. 106 (2008) 628–637.
[25] L.R. Webster, K.L. Fakata, S. Charapata, R. Fisher, M. MineHart, Open-label, multicenter study of combined intrathecal morphine and ziconotide: addition of morphine in patients receiving ziconotide for severe chronic pain, Pain Med. 9 (2008) 282–290.
[26] T. Sakurada, T. Komatsu, S. Sakurada, Mechanisms of nociception evoked by intrathecal high-dose morphine, Neurotoxicology 26 (2005).
[27] S. Mercadante, R.K. Portenoy, Opioid poorly-responsive cancer pain, J. Pain Symptom Manage. 21 (2001).
[28] S. Mercadante, P. Ferrera, P. Villari, E. Arcuri, Hyperalgesia: an emerging iatrogenic syndrome, J. Pain Symptom Manage. 26 (2003).
[29] J.E. Shaw, R.A. Sicreea, P.Z. Zimmet, Global estimates of the prevalence of diabetes for 2010 and 2030, Diabetes Res. Clin. Pract. 87 (2010) 4–14.
[30] International Diabetes Federation, IDF Diabetes Atlas, 4th ed., 2009 http://www.diabetesatlas.org.
[31] J.P. Boyle, T.J. Thompson, E.W. Gregg, L.E. Barker, D.F. Williamson, Projection of the year 2050 burden of diabetes in the US adult population: dynamic modeling of incidence, mortality, and prediabetes prevalence, Popul. Health Metr. 8 (2010) 29.
[32] Report of the expert committee on the diagnosis and classification of diabetes mellitus, Diabetes Care 20 (1997) 1183–1197.
[33] Follow-up report on the diagnosis of diabetes mellitus — the expert committee on the diagnosis and classification of diabetes mellitus, Diabetes Care 26 (2003) 3160–3167.
[34] The Diabetes Control and Complications Trial Research Group, The effect of intensive treatment of diabetes on the development and progression of long-term complications in insulin-dependent diabetes mellitus, N. Engl. J. Med. 329 (1993) 977–986.
[35] UK Prospective Diabetes Study (UKPDS) Group, Intensive blood-glucose control with sulphonylureas or insulin compared with conventional treatment and risk of complications in patients with type 2 diabetes (UKPDS 33), Lancet 352 (1998) 837–853.
[36] J.R. Castle, J.M. Engle, J.E. Youssef, R.G. Massoud, K.C.J. Yuen, R. Kagan, W.K. Ward, Novel use of glucagon in a closed-loop system for prevention of hypoglycemia in type 1 diabetes, Diabetes Care 33 (2010) 1282–1287.
[37] S.L. Aronoff, K. Berkowitz, B. Shreiner, L. Want, Glucose metabolism and regulation: beyond insulin and glucagon, Diabetes Spectr. 17 (2004) 183–190.
[38] S.J. Hassenbusch, R.K. Portenoy, M. Cousins, E. Buchser, T.R. Deer, S.L.D. Pen, J. Eisenach, K.A. Follett, K.R. Hildebrand, E.S. Krames, R.M. Levy, P.P. Palmer, J.P. Rathmell, R.L. Rauck, P.S. Staats, L. Stearns, K.D. Willis, Polyanalgesic Consensus Conference 2003: an update on the management of pain by intraspinal drug delivery — report of an expert panel, J. Pain Symptom Manage. 27 (2004).
[39] E.S. Krames, Practical issues when using neuraxial infusion, Oncology 13 (1999).
[40] T.S. Grabow, D. Derdzinski, P.S. Staats, Spinal drug delivery, Curr. Pain Headache Rep. 5 (2001).
[41] V.C. Anderson, K.J. Burchiel, A prospective study of long-term intrathecal morphine in the management of chronic nonmalignant pain, Neurosurgery 44 (1999).
[42] American Society of Health System Pharmacists, ASHP guidelines on quality assurance for pharmacy-prepared sterile products, Am. J. Health Syst. Pharm. 57 (2000).
[43] D.W. Coombs, N. Fine, Spinal anesthesia using subcutaneously implanted pumps for intrathecal drug infusion, Anesth. Analg. 73 (1991).

[44] Medtronic IsoMed Constant Flow Intrathecal Drug Delivery Pump, http://professional.medtronic.com/pt/neuro/idd/prod/isomed/index.htm, Accessed Aug. 2011.
[45] CODMAN 3000 pump, http://www.codmanpumps.com/, Accessed Aug. 2011.
[46] Medtronic SynchroMed II intrathecal drug delivery pump, http://professional.medtronic.com/pt/neuro/idd/prod/synchromed-ii/index.htm, Accessed Aug. 2011.
[47] Medtronic SynchroMed EL intrathecal drug delivery pump, http://professional.medtronic.com/pt/neuro/idd/prod/synchromed-el/index.htm, Accessed Aug. 2011.
[48] A.T. Evans, S. Chiravuri, Y.B. Gianchandani, A low power, microvalve regulated architecture for drug delivery systems, Biomed. Microdevices 12 (2010) 159–168.
[49] A.T. Evans, Valve Regulated Implantable Drug Delivery for Chronic Pain Management, Ph.D. Thesis, University of Michigan, Ann Arbor, MI, USA, 2010.
[50] E.B. Lobato, N. Gravenstein, R.R. Kirby, Complications in Anesthesiology, Lippincott Williams & Wilkins, 2007.
[51] Current diabetes insulin pumps and comparison chart, http://www.diabetesnet.com/diabetes-technology/insulin-pumps/current-pumps/pump-comparison, Accessed Aug. 2011.
[52] Medtronic MiniMed paradigm revel insulin pump, http://www.minimed.com/, Accessed Jun. 2011.
[53] OneTouch Ping, http://www.animas.com/animas-insulin-pumps/onetouch-ping, Accessed Aug. 2011.
[54] OmniPod insulin pump, http://www.myomnipod.com/, Accessed Jun. 2011.
[55] Sooil Dana Diabecare insulin pumps, http://www.sooil.com/, Accessed Jun. 2011.
[56] Deltec Cozmo insulin pump, http://www.smiths-medical.com/landing-pages/promotions/md/coz-home.html, Accessed Jul. 2011.
[57] ACCU-CHEK Spirit Insulin Pump, http://www.accu-chekinsulinpumps.com/ipus/products/insulinpumps/index.html, Accessed Jul. 2011.
[58] Spring Zone Insulin Pump, http://www.springnow.com, Accessed Aug. 2011.
[59] Pancreum artificial pancreas system, http://www.pancreum.com, Accessed Aug. 2011.
[60] GlobalData, insulin pump world market briefing, http://www.mtbeurope.info/content/ft1008001.htm, Aug. 2010.
[61] A.T. Evans, S. Chiravuri, Y.B. Gianchandani, A multidrug delivery system using a piezoelectrically actuated silicon valve manifold with embedded sensors, IEEE/ASME J. Microelectromech. Syst. 20 (2011) 231–238.
[62] Y. Shinozawa, T. Abe, T. Kondo, A proportional microvalve using a bi-stable magnetic actuator, Proceedings of the IEEE International Conference on Micro Electro Mechanical Systems (MEMS), 1997, pp. 233–237.
[63] C. Fu, Z. Rummler, W. Schomburg, magnetically driven micro ball valves fabricated by multilayer adhesive film bonding, J. Micromech. Microeng. 13 (2003).
[64] P. Dubois, B. Guldimann, N.F.d. Rooij, High-speed electrostatic gas microvalve switching behavior, Proc. SPIE 4560 (2001).
[65] C.A. Rich, K.D. Wise, A high-flow thermopneumatic microvalve with improved efficiency and integrated state sensing, IEEE/ASME J. Microelectromech. Syst. 12 (2003).
[66] S. Messner, M. Muller, V. Burger, J. Schaible, H. Sandmaier, R. Zengerle, A normally-closed, bimetallically actuated 3-way microvalve for pneumatic applications, Proceedings of the IEEE International Conference on Micro Electro Mechanical Systems (MEMS), 1998, pp. 40–44.
[67] M. Kohl, D. Dittmann, E. Quandt, B. Winzek, Thin film shape memory microvalves with adjustable operation temperature, Sensor Actuat .A-Phys. 83 (2000).
[68] M. Esashi, S. Shoji, A. Nakano, Normally closed microvalve and micropump fabricated on a silicon wafer, Sensor Actuat .A-Phys. 20 (1989).
[69] X. Yang, A. Holke, S.A. Jacobson, J.H. Lang, M.A. Schmidt, S.D. Umans, An electrostatic, on/off microvalve designed for gas fuel delivery for the MIT microengine, IEEE/ASME J. Microelectromech. Syst. 13 (2004) 660–668.
[70] I. Chakraborty, W.C. Tang, D.P. Bame, T.K. Tang, MEMS micro-valve for space application, Sensor Actuat .A-Phys. 83 (2000).
[71] D.C. Roberts, L. Hanqing, J.L. Steyn, O. Yaglioglu, S.M. Spearing, M.A. Schmidt, N.W. Hagood, A piezoelectric microvalve for compact high-frequency, high-differential pressure hydraulic micropumping systems, IEEE/ASME J. Microelectromech. Syst. 12 (2003).
[72] T.R. Brosten, J.M. Park, A.T. Evans, K. Rasmussen, G.F. Nellis, S.A. Klein, J.R. Feller, L. Salerno, Y.B. Gianchandani, A numerical flow model and experimental results of a cryogenic micro-valve for distributed cooling applications, Cryogenics 47 (2007) 501–509.
[73] J.M. Park, A.T. Evans, K. Rasmussen, T.R. Brosten, G.F. Nellis, S.A. Klein, Y.B. Gianchandani, A microvalve with integrated sensors and customizable normal state for low temperature operation, IEEE/ASME J. Microelectromech. Syst. 18 (2009) 868–879.
[74] B. Magnes, Body position and cerebrospinal fluid pressure. Part I: clinical studies on the effect of rapid postural changes, J. Neurosurg. 44 (1976) 687–697.
[75] Medtronic, Medtronic SynchroMed II Programmable Infusion System Implant Manual, http://professional.medtronic.com/wcm/groups/mdtcom_sg/@mdt/@neuro/documents/documents/pump-ii8637-impmanl.pdf, 2003.
[76] R. Hovorka, Continuous glucose monitoring and closed-loop systems, Diabet. Med. 23 (2006) 1–12.
[77] J.J. Mastrototaro, K.W. Cooper, G. Soundararajan, J.B. Sanders, R.V. Shah, Clinical experience with an integrated continuous glucose sensor/insulin pump platform: a feasibility study, Adv. Ther. 23 (2006) 725–732.
[78] I.B. Hirsch, J. Abelseth, B.W. Bode, J.S. Fischer, F.R. Kaufman, J. Mastrototaro, C.G. Parkin, H.A. Wolpert, B.A. Buckingham, Sensor-augmented insulin pump therapy: results of the first randomized treat-to-target study, Diabetes Technol. Ther. 10 (2008) 377–383.
[79] J.L.C. Clark, C. Lyons, A.N.Y. Aead, Electrode systems for continuous monitoring in cardiovascular surgery, Science 102 (1962) 29–45.
[80] G. Reach, G.S. Wilson, Can continuous glucose monitoring be used for the treatment of diabetes, Anal. Chem. 64 (1992) 381A–386A.
[81] A.P.F. Turner, B. Chen, S.A. Piletsky, In vitro diagnostics in diabetes: meeting the challenge, Clin. Chem. 45 (1999) 1596–1601.
[82] P.T. Kissinger, Biosensors—a perspective, Biosens. Bioelectron. 20 (2005) 2512–2516.
[83] J.D. Newman, A.P.F. Turner, Home blood glucose biosensors: a commercial perspective, Biosens. Bioelectron. 20 (2005) 2435–2453.
[84] F. Ricci, G. Palleschi, Sensor and biosensor preparation, optimisation and applications of Prussian Blue modified electrodes, Biosens. Bioelectron. 21 (2005) 389–407.
[85] G.S. Wilson, R. Gifford, Biosensors for real-time in vivo measurements, Biosens. Bioelectron. 20 (2005) 2388–2403.
[86] J.C. Pickup, F. Hussain, N.D. Evans, N. Sachedina, In vivo glucose monitoring: the clinical reality and the promise, Biosens. Bioelectron. 20 (2005) 1897–1902.
[87] J. Wang, Electrochemical glucose biosensors, Chem. Rev. 108 (2008) 814–825.
[88] R. Wilson, A.P.F. Turner, Glucose oxidase: an ideal enzyme, Biosens. Bioelectron. 7 (1992) 165–185.
[89] E. Shoji, M.S. Freund, Potentiometric sensors based on the inductive effect on the pKa of poly(aniline): a nonenzymatic glucose sensor, J. Am. Chem. Soc. 123 (2001) 3383–3384.
[90] S. Park, H. Boo, T.D. Chung, Electrochemical nonenzymatic glucose sensors, Anal. Chim. Acta 556 (2006) 46–57.
[91] T.G.S. Babu, T. Ramachandran, B. Nair, Single step modification of copper electrode for the highly sensitive and selective non-enzymatic determination of glucose, Microchim. Acta 169 (2010) 49–55.
[92] T.G.S. Babu, P.V. Suneesha, T. Ramachandrana, B. Nair, Gold nanoparticles modified titania nanotube arrays for amperometric determination of ascorbic acid, Anal. Lett. 43 (2010) 2809–2822.
[93] T.G.S. Babu, T. Ramachandrana, Development of highly sensitive non-enzymatic sensor for the selective determination of glucose and fabrication of a working model, Electrochim. Acta 55 (2010) 1612–1618.
[94] M. Carmichael, The changing science of pain, Newsweek, Jun. 4, 2007.
[95] B.R. Boveja, A. Widhany, Method and system for providing pulsed electrical stimulation to provide therapy for erectile/sexual dysfunction, prostatitis, prostatitis pain, and chronic pelvic pain, U.S. Patent No. 7,330,762, 2008.
[96] R. Vipul, Vipul's lifetime lifeline permanent pacemaker and implantable cardioverter-defibrillator, U.S. Patent No. 7,239,917, 2007.
[97] D. Reynaerts, J. Peirs, H.V. Brussel, A SMA-actuated implantable system for delivery of liquid drugs, Proceedings of the Fifth International Conference on New Actuators, 1996.
[98] J.C. Andrews, S.C. Walker-Andrews, W.D. Ensminger, Long-term central venous access with a peripherally placed subcutaneous infusion port: initial results, Radiology 176 (1990).
[99] S. Strum, J. McDermed, A. Korn, C. Joseph, Improved methods for venous access: the Port-A-Cath, a totally implanted catheter system, J. Clin. Oncol. 4 (1986).
[100] S.L. Morris, P.F. Jaques, M.A. Mauro, Radiology-assisted placement of implantable subcutaneous infusion ports for long-term venous access, Radiology 184 (1992).
[101] A.T. Evans, S. Chiravuri, Y. Gianchandani, Transdermal power transfer for recharging implanted drug delivery devices via the refill port, Biomed. Microdevices 12 (2010) 179–185.
[102] H. Kim, K. Najafi, Characterization of low-temperature wafer bonding using thin-film Parylene, IEEE/ASME J. Microelectromech. Syst. 14 (2005) 1347–1355.
[103] R. Hovorka, J.M. Allen, D. Elleri, L.J. Chassin, J. Harris, D. Xing, C. Kollman, T. Hovorka, A.M.F. Larsen, M. Nodale, A. De Palma, M.E. Wilinska, C.L. Acerini, D.B. Dunger, Manual closed-loop insulin delivery in children and adolescents with type 1 diabetes: a phase 2 randomised crossover trial, Lancet 375 (2010) 743–751.
[104] D. Bruttomesso, A. Farret, S. Costa, M.C. Marescotti, M. Vettore, A. Avogaro, A. Tiengo, C.D. Man, J. Place, A. Facchinetti, S. Guerra, L. Magni, G.D. Nicolao, C. Cobelli, E. Renard, A. Maran, Closed-loop artificial pancreas using subcutaneous glucose sensing and insulin delivery and a model predictive control algorithm: preliminary studies in Padova and Montpellier, J. Diabetes Sci. Technol. 3 (2009) 1014–1021.
[105] The bionic pancreas for type I diabetics, http://www3.imperial.ac.uk/bioinspiredtechnology/research/bionicpancreas, Accessed Aug. 2011.